analytical chemistry

Article

pubs.acs.org/ac

Chromatographic Enrichment and Subsequent Separation of Nickel and Vanadyl Porphyrins from Natural Seeps and Molecular Characterization by Positive Electrospray Ionization FT-ICR Mass Spectrometry

Jonathan C. Putman,[†,§] Steven M. Rowland,[†,‡] Yuri E. Corilo,[†,§] and Amy M. McKenna*[,†]

[†]National High Magnetic Field Laboratory and [§]Future Fuels Institute, Florida State University, 1800 East Paul Dirac Drive, Tallahassee, Florida 32310-4005, United States

[‡]Department of Chemistry and Biochemistry, 95 Chieftain Way, Florida State University, Tallahassee, Florida 32306, United States

Supporting Information

ABSTRACT: We report a novel chromatographic method to enrich and separate nickel and vanadyl porphyrins from a natural seep sample and combine molecular level characterization by positive-ion electrospray ionization Fourier transform ion cyclotron resonance mass spectrometry (FT-ICR MS). Vanadyl and nickel porphyrin model compound elution from primary secondary amine (PSA) stationary phase combined with UV-vis spectroscopy confirms enrichment and subsequent fractionation of nickel and vanadyl porphyrins into polarity-based subfractions. A more than 100-fold increase in signal-to-noise ratio for nickel porphyrins enables unequivocal elemental composition assignment confirmed by isotopic fine structure for all isotopes >1% relative abundance, and the first mass spectral identification of ^{61}Ni porphyrin isotopologues derived from natural seeps. Oxygen-containing vanadyl porphyrins and sulfur-containing vanadyl porphyrins are isolated in the same fraction simultaneously from the same sample. We provide the first chromatographic evidence of carboxylic acid functionalities peripheral to the porphyrin core, in agreement with previous studies.

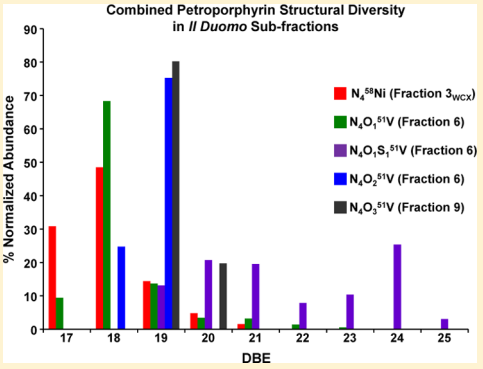

Vanadium and nickel porphyrins are the most abundant metal-containing compounds in crude oil and the first molecules that linked petroleum to its biological origin in the 1930s by Alfred Treibs.[1,2] Porphyrins are degradation products of biological pigments (i.e., algal and bacterial chlorophylls and hemoglobin),[3] and chromatographic distribution profiles correlate to deposition environment and thermal history of sedimentary deposits.[4−6] Oil composition, geological origin, and depositional environment contribute to variations in vanadium and nickel concentration.[4,7] The concentration of nickel and vanadium increases with viscosity, with reported vanadium concentrations >1200 ppm.[8] Heavily degraded, weathered oil derived from natural seepage represents the most complex natural organic mixture to date, and previous studies catalogue the structural diversity of nickel and vanadyl porphyrins detected directly by FT-ICR mass spectrometry in natural seeps at Coal Oil Point in the Santa Barbara Channel, California.[9] However, the complex hydrocarbon matrix challenges direct identification of a wide range of porphyrin structural classes.

Nickel and vanadyl porphyrins abundant in crude oil exist as homologous series of a few major structural classes,[10,11] although more than 80 different porphyrins have been identified from organic-rich sediments and crude oils.[4,11] The porphyrin carbon skeleton consists of a tetrapyrrolic, planar, cyclic molecule linked with methine bridges,[1,11] and etioporphyrins are the simplest structural class, with ethyl and methyl substitution at the Cβ position on each pyrrole.[4,12] Structures of nickel and vanadyl porphyrins have been characterized by X-ray crystallography[13] and vibrational spectroscopy.[14]

Vanadium and nickel porphyrin chemical and physical properties have been studied extensively[15] based on enrichment and isolation strategies[16,17] and mass spectral analysis.[10,18−21] The main porphyrin structures identified in petroleum correspond to etioporphyrin (Etio) and deoxophylloerythroetioporphyrin (DPEP) structure complexes in nickel and vanadyl forms,[1,2] and recent reports have identified sulfur- and oxygen-containing porphyrins.[4,5,17,22] Chromatographic isolation of vanadyl and nickel porphyrins from heavy crude oil combined with FT-ICR mass spectrometry identified sulfur- and oxygen-containing porphyrins by reducing interferences from the complex hydrocarbon matrix.[17,23] However, these methods focus on enrichment of all porphyrins, with little separation between type and structural class.

The immense compositional complexity and increased polarity associated with heavily degraded natural petroleum

Received: July 14, 2014
Accepted: October 6, 2014
Published: October 6, 2014

seeps challenge nearly all routine analytical techniques. Fourier transform ion cyclotron resonance mass spectrometry can address the compositional complexity of heavy crude oil at the molecular level.[24] Because vanadyl and nickel porphyrins concentrate in heavy oils, previous studies rely on atmospheric pressure photoionization (APPI) coupled to FT-ICR MS to identify nickel and vanadyl porphyrins at the molecular level.[9,19,20,22] However, positive-ion APPI yields protonated ions and radical cations for each neutral molecule and produces two mass spectral peaks per neutral analyte molecule. APPI FT-ICR mass spectral characterization of asphalt volcanoes in Southern California reported more than 85 000 unique elemental compositions and catalogued the structural diversity of nickel and vanadyl porphyrins in the same sample.[9] However, direct identification of vanadyl and nickel porphyrins in a whole, unfractionated sample is limited to the most abundant porphyrin compounds due to low ionization efficiency and dynamic range limitations.

Previous separation methods to target petroporphyrins combine normal phase fractionation on silica and/or alumina stationary phase, followed by elution with mobile phase of increasing solvent strength, but result in coelution of nickel and vanadium porphyrins.[17,21] Xu et al. performed an online HPLC separation to improve selectivity with amino propyl silica[25] and separated nickel and vanadyl porphyrins and isomers on a chromatographic time scale. The nonplanar structure and lone pairs of electrons on the oxygen atom increase the hydrogen bonding capabilities for vanadyl porphyrins and result in increased retention.[25]

Mass spectral identification of novel petroporphyrin structural classes has been based on separation and enrichment strategies to simplify the complex hydrocarbon matrix. Shi et al. combined chromatographic fractionation with electrospray ionization (ESI) FT-ICR mass spectrometry and identified three new series of oxygenated vanadyl porphyrins.[17] Qian et al. applied cyclograph enrichment to identify nickel porphyrins[19] and solubility enrichment to identify sulfur-containing vanadyl porphyrins[20] and combined with positive-ion atmospheric pressure photoionization (APPI) FT-ICR mass spectrometry identified petroporphyrins contained in each subfraction, as previously reported.[9,22] However, the multiple ionization pathways possible in APPI increase spectral complexity and require resolving power ($m/\Delta m_{50\%}$, where $\Delta m_{50\%}$ is the mass spectral peak width at half-maximum peak height) $m/\Delta m_{50\%} > 1\,000\,000$[9] to resolve isobaric overlaps critical for accurate elemental composition assignment.[19]

Rodgers et al. first applied positive-ion electrospray ionization to petroporphyrin-enriched chromatographic fractions and identified monomer and dimer porphyrin species.[21] Dopant-assisted APPI[26] produces ions from nonpolar and polar compounds through charge-exchange and proton transfer reactions, whereas electrospray ionization produces protonated cations from polar species through solution-based protonation reactions.[27] Moreover, ESI selectively ionizes the most polar compounds and yields one ion for every neutral, compared to APPI, which requires higher resolving power to identify isobaric species due to multiple ionization pathways that produce a more complex mass spectrum. Here we combine targeted enrichment and chromatographic separation of vanadyl and nickel porphyrins with positive-ion electrospray ionization FT-ICR MS to highlight the structural diversity of porphyrins inherent in natural seep samples. To the best of our knowledge, this represents the first molecular catalogue of nickel and vanadyl porphyrins separated in chromatographic space and characterized at the molecular level confirmed with isotopic fine structure.

EXPERIMENTAL METHODS

Sample Description. A previously studied asphalt volcano sample[9,28] (Il Duomo (#4332-1)) with 514 (±2) ppm vanadium and 158 (±2) ppm nickel was collected as chunks of oil and sand and extracted with toluene in a Soxhlet extractor.

Materials. HPLC-grade solvents (hexanes (95% *n*-hexane, CAS no. 110-54-3), toluene (CAS no. 108-88-3), and methanol (CAS no. 67-56-1)) were purchased from J.T. Baker/Avantor Performance Materials (Center Valley, PA). Reagent grade formic acid (CAS no. 64-18-6, ≥95%), 2,3,7,8,12,13,17,18-octaethyl-21*H*,23*H*-porphine vanadium(IV) oxide ($C_{36}H_{44}N_4OV$, CAS no. 27860-55-5, V=O(IV)OEP), and 2,3,7,8,12,13,17,18-octaethyl-21*H*,23*H*-porphine nickel(II) ($C_{36}H_{44}N_4Ni$, CAS no. 24803-99-4, Ni(II)OEP) were purchased from Sigma-Aldrich Chemical Co. (St. Louis, MO). Chromatographic fractionation conducted on primary secondary amine (PSA) solid-phase extraction (SPE) cartridges (Bond Elut Plexa; Mega BE-PSA, 2 g/12 mL, PSA; 40 μm, 60A; Agilent Technologies, Santa Clara, CA) followed by secondary purification with a weak cation exchange (WCX) SPE cartridge (Phenomenex Strata WCX; 55um 70 A; 1 g/6 mL, Phenomenex, Torrance, CA).

Sample Preparation. Stock solutions of V=O(IV)OEP and Ni(II)OEP (2 μM) were prepared in 1:1 (by volume) hexane/toluene. Whole chunks of Il Duomo were finely ground in a mortar and pestle, extracted with toluene (~12 h), and desolvated with dry N_2, and chromatographic fractions were collected and desolvated. Extracts and fractions were dissolved in toluene to yield stock solutions (1 mg/mL) and further diluted in toluene with equal parts (vol:vol) methanol spiked with 10% (by volume) formic acid to a final concentration of 10−50 μg/mL prior to analysis. Total percent yield for whole Il Duomo extract (i.e., asphaltenes and maltenes) is shown in Table S-1, Supporting Information.

UV−Visible Spectroscopic Analysis. UV−vis spectroscopy (Agilent 8453, Agilent Technologies, Santa Clara, CA) identified petroporphyrins within Il Duomo subfractions. A UV−vis spectrophotometer equipped with a 1 cm cuvette and HPLC-grade toluene was used, scanning from 300 to 700 nm. Three classical absorptions that arise from the allowed $\pi-\pi^*$ transitions occur in porphyrins: a strong β-band (Soret band) in the violet region (390−410 nm) and two weaker bands (α and β) in the yellow-green region (500−580 nm).[4,29] Nickel porphyrin absorptions blue-shift to slightly lower wavelength, due to the increased planarity of the porphyrin macrocycle.[30]

Ionization: ESI Source. Sample solutions were infused via a microelectrospray source[31] (50 μm i.d. fused silica emitter) at 500 nL/min by a syringe pump. Ions formed at atmospheric pressure enter through a dual-stage rf-focusing ion funnel interface[32] (funnel 1:2.7 Torr; funnel 2:270 mTorr) with a voltage gradient transfer of ions into the mass spectrometer (DC1 = 120 V; DC2 = 70 V; DC3 = 40 V; DC4 = 10 V).

9.4 T FT-ICR Mass Spectrometer. Whole Il Duomo extract and chromatographic fractions were analyzed with a custom-built FT-ICR mass spectrometer[33] equipped with a 9.4 T horizontal 220 mm bore diameter superconducting solenoid magnet operated at room temperature and a modular ICR data station (Predator)[34] facilitated instrument control, data

dx.doi.org/10.1021/ac502672b | Anal. Chem. 2014, 86, 10708−10715

acquisition, and data analysis. Due to increased complexity at higher m/z, broadband phase correction[35] was applied to mass spectra for seep extracts and fractions to increase the resolution of isobaric species as previously described.[36] For all mass spectra, the achieved mass spectral resolving power approached the theoretical limit[37] across the entire mass range, e.g., average resolving power, $m/\Delta m_{50\%}$, in which $\Delta m_{50\%}$, the mass spectral peak width at half-maximum peak height, was ~1 000 000−1 500 000 at m/z 500. Additional information for data processing, mass calibration, and data analysis are detailed in Supporting Information.

RESULTS AND DISCUSSION

Porphyrin Standard Analysis. PSA stationary phase, a silica-based ethylenediamine-*N*-propyl sorbent, provides both primary- and secondary-amine functionalities that retain both nickel and vanadyl porphyrin model compounds for subsequent separation, likely due to chelation properties of the bidentate diamine functionality.[38] PSA solid-phase extraction (SPE) cartridges were preconditioned with ~12 mL of hexane. Model compounds were dissolved in toluene and diluted with hexane to a final concentration of 2 μM, and a 1 mL aliquot was loaded onto a SPE cartridge and allowed to equilibrate (15 min). Sequential elution began with pure hexane, and the concentration of toluene was increased stepwise in small increments (5−10% by volume). Band broadening of Ni(II)OEP that was observed on aminopropyl silica (APS) was not observed on PSA and remained in a narrow band (see Figure S-1, Supporting Information). The nickel band does not begin to migrate until the mobile phase composition reaches 15−20% toluene. V=O(IV)OEP remains in a narrow, uniform band, and migration occurs when the mobile phase composition exceeds 60% toluene by volume and elutes completely with 70% toluene.

Petroporphyrin Fraction Analysis. Figure 1 shows the separation scheme based on elution profiles of model compounds (Ni(II)OEP and VO-OEP). Whole Il Duomo extract was dissolved in 500 μL of toluene and further diluted with 500 μL of hexane, loaded dropwise onto the preconditioned PSA SPE cartridge, and allowed to equilibrate (~15 min). Fraction 1 contains the compounds that do not

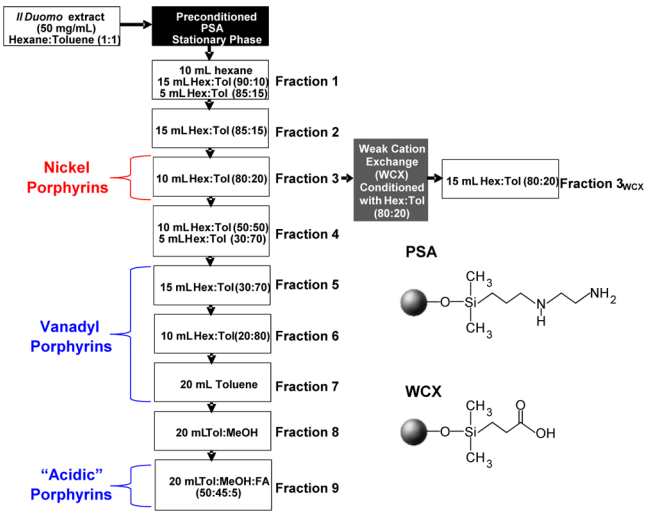

Figure 1. Separation scheme employed to isolate petroporphyrin fractions from Il Duomo toluene extract.

interact with the polar stationary phase (i.e., hydrocarbons, saturated compounds) and elute in three steps: 10 mL of hexane, 15 mL of 90:10 hexane:toluene (v/v), and 5 mL of 85:15 hexane:toluene (v/v). Elution with 15 mL of 85:15 hexane:toluene (v/v) yields fraction 2, which shows slight absorption at the Soret band, but an increase to 80:20 hexane:toluene (v/v) elutes nickel porphyrins. Both fractions contain nickel porphyrins, but fraction 3 shows absorption at the nickel α-band. The nickel porphyrin-containing fraction (fraction 3) was passed through a weak cation exchange (WCX) sorbent with an isocratic mobile phase composed of 80:20 hexane:toluene (v/v) for further purification. Table S-1 (Supporting Information) shows the percent yield across all PSA fractions, with a total percent recovery of 87% for the whole Il Duomo sample (i.e., asphaltenes and maltenes). Replicate fractionations of Il Duomo, a terrestrial seep, and an asphaltene verified reproducibility and will be expanded in future studies. In all cases, more than 100 different types of porphyrins were identified in the purified porphyrin fractions. For brevity, we report the first replicate of Il Duomo for method validation

Figure 2 shows UV−vis spectra of Il Duomo and subfractions. Three classical metalloporphyrin absorptions

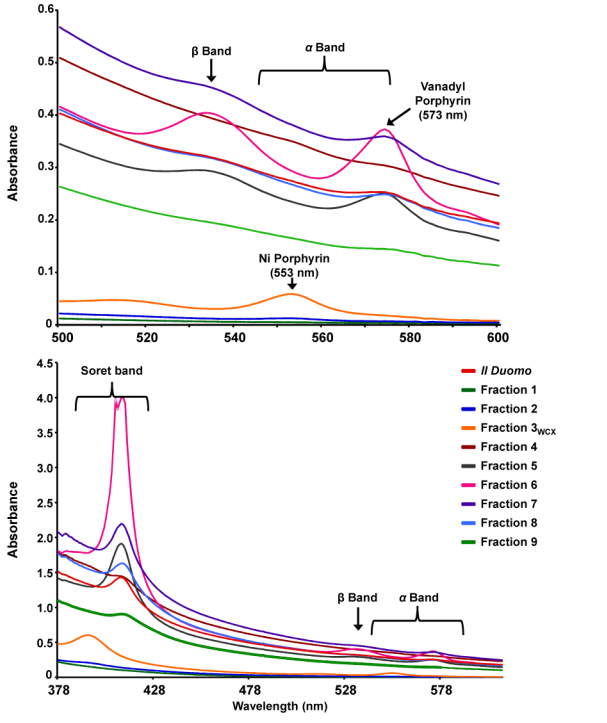

Figure 2. UV−vis spectra of Il Duomo toluene extract and chromatographic subfractions.

arise due to the allowed $\pi-\pi^*$ transitions: a strong Soret band in the violet region (390−410 nm) and two weaker bands (Q0 or α and Q1 or β) in the yellow-green region (500−580 nm).[4,29] Characteristic vanadyl porphyrin absorbance at the Soret band (410 nm), β-band (533 nm), and α-band (572 nm) occurred in the whole extract and fractions 5−7. A blue-shifted nickel Soret band at 393 nm and an α-band at 553 nm were only observed in fraction 3_{WCX}. No porphyrin mass spectral peaks were observed in fraction 4 and no significant absorbance at Soret, α-, or β-bands, which indicates complete separation of nickel and vanadyl porphyrins. Weak absorbance observed for

dx.doi.org/10.1021/ac502672b | Anal. Chem. 2014, 86, 10708−10715

fractions 8 and 9 and elution with formic acid (fraction 9) indicate carboxylic acid-functionalized porphyrins, in agreement with naphthenic acid literature.[39] Quantitation of total vanadium and nickel concentrations in each subfraction will be the focus of future studies.

Heteroatom Class Distributions. Figure 3 shows the class distribution for all heteroatom classes of >0.5% relative abundance derived from positive-ion ESI FT-ICR mass spectra of the whole Il Duomo extract and nickel (fraction 3_{WCX}) and vanadyl (fraction 6) fractions. Figure 3a shows the increased relative abundance of ^{58}Ni and ^{60}Ni porphyrins only detected after weak cation exchange, likely due to reduced matrix effects by removal of easily ionized pyridinic nitrogen and N_1S_x compounds. The nickel porphyrins constitute the seventh most abundant class in fraction 3_{WCX} but were not detected in the whole sample, and only the most abundant nickel porphyrins were detected in fraction 3. Vanadyl porphyrins are detected at >5% relative abundance in fraction 6 but less than 0.5% relative abundance in the whole extract (Figure 3b). The increased relative abundance of vanadyl compared to nickel porphyrins agrees with previous reports of more than three times the total vanadium content in Il Duomo compared to nickel.[9] Vanadyl porphyrins in fraction 6 are selectively ionized in positive mode because they coelute with S_xO_y compounds that have lower ionization efficiency in positive-ion ESI compared with pyridinic nitrogen species that coelute with nickel porphyrins (fraction 3). Nickel porphyrins have also been reported to have ionization efficiencies lower than those of vanadyl porphyrins.[19]

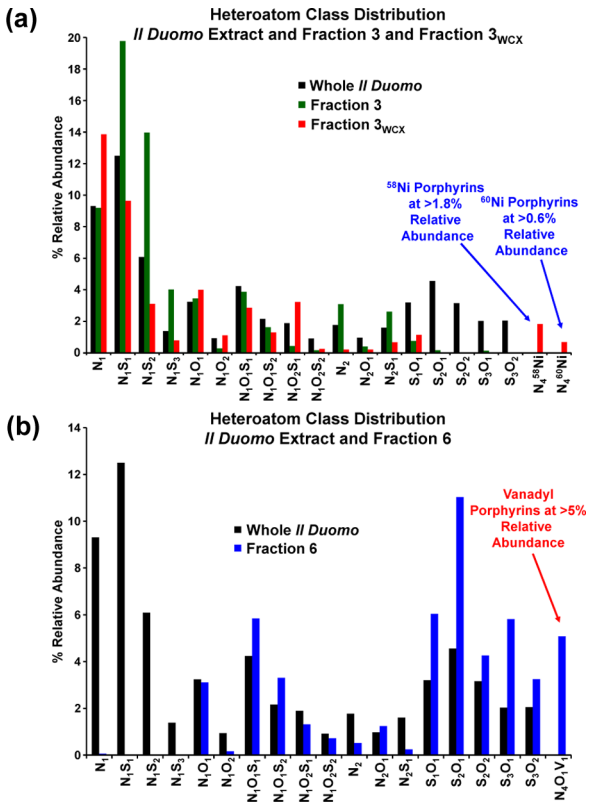

Figure 3. Heteroatom class distribution for whole Il Duomo extract and fraction 3 and fraction 3WCX (top) and fraction 6 (bottom). Nickel porphyrins are observed at >1.8% (^{58}Ni) and >0.6% (^{60}Ni) relative abundance after secondary purification by weak cation exchange (top), and vanadyl porphyrins not detected in the whole extract are observed at >5% relative abundance in fraction 6 (bottom).

ESI FT-ICR MS of Nickel Porphyrin Fractions: Elemental Composition Assignment. Figure 4a shows broadband positive-ion ESI FT-ICR mass spectra of whole Il Duomo (top), fraction 3 (middle), and fraction 3_{WCX} (bottom). More than 17 000 peaks were assigned in the whole sample, and ~10 000 peaks were assigned in fraction 3 and fraction 3_{WCX}. The mass-scale-expanded segment (Figure 4b) for all three spectra at m/z 561 shows a DPEP nickel porphyrin monoisotopic peak at signal-to-noise ratio (S/N) < 5 in the whole sample. After initial fractionation, the same peak is observed at S/N = 35. After weak cation exchange, the DPEP monoisoptopic peak increases 14-fold to S/N ratio = 500, sufficient for elemental composition assignment ($[C_{34}H_{38}N_4{}^{58}Ni+H]^+$ at mass error of −5 ppb).

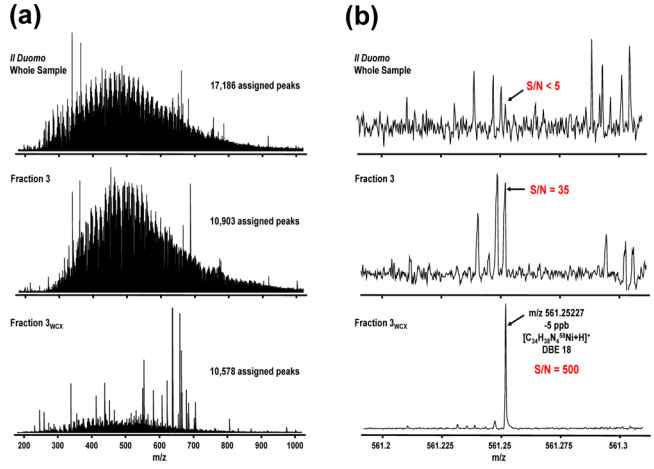

Figure 4. Broadband positive-ion ESI FT-ICR mass spectra of Il Duomo extract (a, top) and fraction 3 before (a, middle) and after secondary purification (a, bottom). A total of 17 186 mass spectral peaks were assigned with signal magnitude greater than 6 times the signal-to-noise ratio baseline root-mean-square (rms) noise in the whole extract and ~10 000 assigned peaks before and after weak cation exchange. Mass-scale-expanded segment at m/z 561 (b) for all three samples highlights the ~100 fold increase in signal-to-noise for an etio nickel porphyrin monoisotopic peak.

Validation of ^{58}Ni Porphyrin Elemental Composition Assignment with ^{60}Ni, ^{61}Ni, ^{62}Ni Isotopologues. Figure 5 shows the mass-scale-expanded segment from fraction 3_{WCX} at $561 < m/z < 566$. The DPEP $[C_{34}H_{38}N_4{}^{58}Ni+H]^+$ (DBE 18) nickel porphyrin monoisotopic peak and corresponding ^{13}C isotopologues at 1.0033 Da higher in mass, ^{60}Ni isotopologue at 1.9954 Da higher in mass, ^{61}Ni at 2.995 Da higher in mass, and ^{62}Ni isotopologue 3.9930 Da higher in mass provide unequivocal confirmation of nickel porphyrin elemental composition assignment. The etio $[C_{34}H_{40}N_4{}^{58}Ni+H]^+$ (DBE 17) nickel porphyrin monoisotopic peaks and corresponding ^{60}Ni isotopologue at 1.9954 Da higher in mass are also shown. All elemental compositions are identified within 100 ppb mass error. Previous identification of ^{62}Ni porphyrin isotopologues relied on APPI ionization.[19] To the best of our knowledge, this is the first mass spectral identification of ^{61}Ni and ^{62}Ni isotopologues of DPEP nickel porphyrin by positive-ion electrospray ionization, and the first identification of ^{61}Ni by any ionization technique. Table S-2 (Supporting Information) lists the elemental composition, the theoretical mass,

dx.doi.org/10.1021/ac502672b | Anal. Chem. 2014, 86, 10708−10715

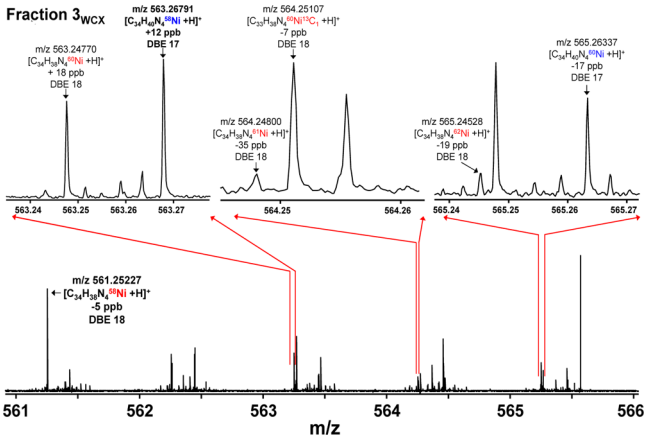

Figure 5. Mass-scale-expanded segments ($561 < m/z < 566$) of the positive-ion ESI FT-ICR mass spectrum of chromatographic fraction 3WCX from Il Duomo toluene extract. The resolution and identification of ^{60}Ni, ^{61}Ni, and ^{62}Ni isotopologues validate elemental composition assignments based on etio and DPEP monoisotopic peaks (see text).

experimental mass, and theoretical and experimental isotopic ratios for the two most abundant nickel porphyrins in fraction 3_{WCX}.

Nickel Porphyrin Elemental Composition Assignment by ESI FT-ICR MS. Figure 6 shows the isoabundance color-

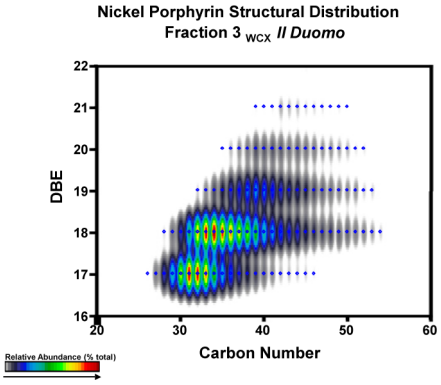

Figure 6. Isoabundance color-contoured plot of double bond equivalents (DBE) versus carbon number for the nickel porphyrin class of fraction 3WCX from Il Duomo toluene extract.

countered plot of DBE versus carbon number for nickel porphyrins identified, with the most abundant compounds corresponding to DBE 17 (Etio) and DBE 18 (DPEP) structural classes, each as a homologous series with carbon number C_{26}–C_{54}. Table S-3a–e (Supporting Information) lists the elemental composition, experimental mass, theoretical mass, mass error, and mass resolving power for each homologous series, with RMS error for each nickel porphyrin series <60 ppb.

ESI FT-ICR MS of Vanadyl Porphyrin Fractions: Elemental Composition Assignment. Figure 7 shows the broadband positive-ion ESI FT-ICR mass spectra of Il Duomo asphalt volcano sample (top) and fraction 6 (bottom). The achieved resolving power of $m/\Delta m_{50\%}$ = 1 300 000 at m/z 550 enables elemental composition assignment to 17 186 mass spectral peaks in Il Duomo (Figure 7a, top) and 9570 in fraction 6 (Figure 7a, bottom), each with signal magnitude

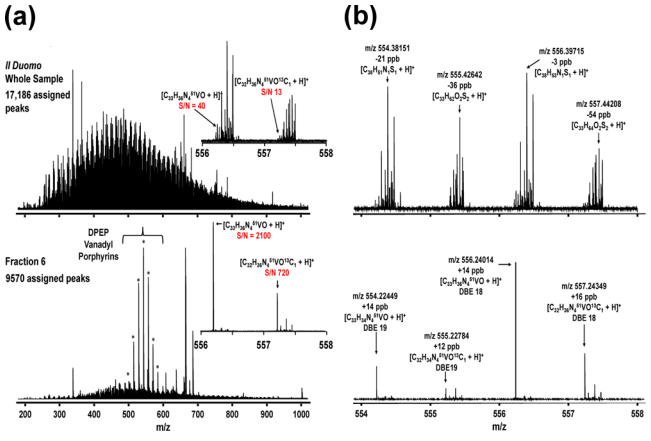

Figure 7. Broadband positive-ion ESI FT-ICR mass spectra of Il Duomo extract (a, top) and fraction 6 (a, bottom). The more than 17 000 mass spectral peaks (each with magnitude greater than 6σ of baseline root-mean-square (rms) noise) were resolved and identified in the whole extract, and 9570 peaks were assigned in fraction 6. Mass-scale-expanded segment at $556 < m/z < 558$ (a) for both samples highlights the ~50 fold increase in signal-to-noise for a DPEP (DBE 18) vanadyl porphyrin monoisotopic peak and its ^{13}C isotopologue at 1.0033 Da higher in mass (a, inset). The most abundant mass spectral peaks in the whole Il Duomo extract correspond to N_1S_1 and O_2S_2 classes (b, top), while DPEP (DBE 18) and Di-DPEP (DBE 19) vanadyl porphyrin monoisotopic peaks and ^{13}C isotopologues are the most abundant compounds in fraction 6 across the same mass range (b, bottom).

greater than 6σ of baseline rms noise (m/z 200–1000). All ions are singly charged, as evident from the unit m/z spacing between species differing by $^{12}C_c$ versus $^{13}C_1{}^{12}C_{c-1}$. Strong vanadyl porphyrin UV–vis absorbance occurs in fraction 6, with weaker absorbance in fractions 5 and 7. Vanadyl porphyrins in fractions 5 and 7 are much lower in abundance and structural diversity. Therefore, we selected the fraction with the strongest UV–vis porphyrin signature (fraction 6) to catalogue vanadyl porphyrin structural diversity. DPEP vanadyl porphyrins ($C_nH_{2n-30}N_4V_1O_1$) are the most abundant porphyrin class, in agreement with previous reports.[9,21,22] Mass zoom insets at $556 < m/z < 558$ (Figure 7a, inset) highlight the 50-fold increase in signal-to-noise ratio for DPEP vanadyl porphyrins in fraction 6 compared to whole Il Duomo.

Figure 7b shows the mass-scale-expanded segment at m/z 554–558 for Il Duomo (Figure 7b, top) and fraction 6 (Figure 7b, bottom). Mass spectral peaks with highest signal magnitude correspond to nonporphyrinic petroleum compounds in the whole sample (top) based on elemental composition assignment. Across the same m/z range, the most abundant mass spectral peaks correspond to vanadyl porphyrins and isotopologues after fractionation. A DBE value of 18 corresponds to a DPEP ($C_nH_{2n-30}N_4V_1O_1$) structure that is most abundant, and Di-DPEP structure ($C_nH_{2n-28}N_4V_1O_1$) corresponds to DBE 19, in agreement with previous reports.[21,22] The increased signal-to-noise ratio after PSA fractionation enables identification of >90 unique elemental compositions that correspond to vanadyl porphyrins (Table S-4a–g, Supporting Information). The rms error for each homologous series ranged between 8 and 60 ppb.

Vanadyl Porphyrin Structural Diversity. Figure 8 shows the isoabundance color-contoured plot of DBE versus carbon number for vanadyl porphyrins identified in fraction 6, with the most abundant structures corresponding to DPEP (DBE = 18).

dx.doi.org/10.1021/ac502672b | Anal. Chem. 2014, 86, 10708–10715

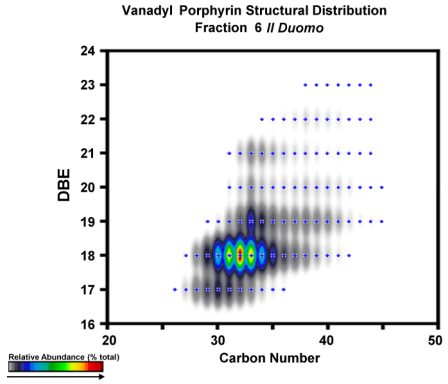

Figure 8. Isoabundance color-contoured plot of double bond equivalents (DBE) versus carbon number for the vanadyl porphyrin class of fraction 6 from Il Duomo toluene extract.

Vanadyl porphyrins with DBE = 17−23 were also observed with carbon number distributions between C_{25} and C_{45}.

Sulfur-Containing Vanadyl Porphyrins. Qian et al. first identified sulfur-containing vanadyl porphyrins by APPI FT-ICR MS in asphaltenes (*n*-heptane insoluble) derived from vacuum residue and proposed benzothiophene sulfur addition to etio porphyrin core structures.[20] More than 60 unique elemental compositions that correspond to sulfur-containing vanadyl porphyrins were identified and assigned in fraction 6. Figure 9 shows the isoabundance contour plot of DBE versus

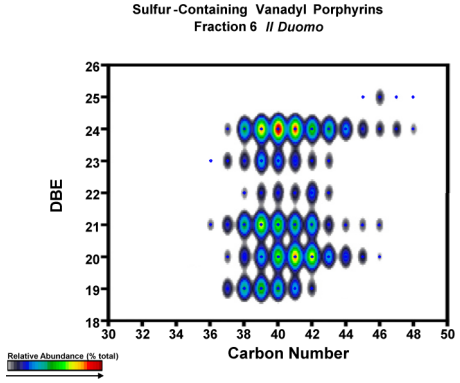

Figure 9. Isoabundance color-contoured plot of double bond equivalents (DBE) versus carbon number for the sulfur-containing vanadyl porphyrin class of fraction 6 from Il Duomo toluene extract.

carbon number for sulfur-containing vanadyl porphyrins, with DBE 19−25 and carbon number ∼C_{35}−C_{48}. The most abundant structural class corresponds to DBE 24. Qian et al. reported that the most abundant sulfur-vanadyl porphyrins increased in *z*-number by ∼10, which converts to approximately 5−6 DBE, and postulated benzothiophene addition to etio vanadyl porphyrin cores.[20] The most abundant Il Duomo vanadyl porphyrins (DBE 18) and sulfur-vanadyl porphyrins (DBE 24) could occur through benzothiophene addition. (Table S-5a−g, Supporting Information) Structural interrogation of these compounds will be the focus of future work.[20]

Oxygen-Containing Vanadyl Porphyrins. Zhao et al. first identified oxygenated vanadyl porphyrins by positive-ion electrospray FT-ICR MS characterization of chromatographic fractions derived from Venezuelan heavy crude and reported three new vanadyl porphyrin structural classes ($C_cH_hN_4VO_2$, $C_cH_hN_4VO_3$, and $C_cH_hN_4VO_4$) that were proposed to incorporate ketone, aldehyde, and carboxylic acid moieties to known porphyrin core structures.[17] Figure 10 shows the DBE

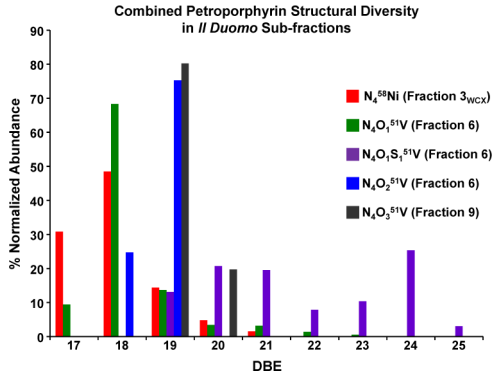

Figure 10. Combined normalized DBE distribution for $N_4{}^{58}Ni$, $N_4O_1{}^{51}V$, $N_4O_1S_1{}^{51}V$, $N_4O_2{}^{51}V$, and $N_4O_3{}^{51}V$ porphyrin classes observed within fractions 3_{WCX} and fractions 6 and 9.

distribution for all porphyrin classes identified after chromatographic fractionation. The percent relative abundance for each class was normalized to 100% total abundance for each class. The addition of one oxygen atom ($N_4O_2{}^{51}V$) corresponds to DBE values of 18 and 19, which indicates preferential incorporation of ketone/aldehyde functionalities to etio and DPEP core structures (Table S-6, Supporting Information). The observed increase in DBE and coelution of $N_4O_3{}^{51}V$ porphyrins with naphthenic acids provides mass spectral and chromatographic evidence of carboxylic acid-functionalized vanadyl porphyrins, as previously proposed.[17] $C_cH_hN_4VO_2$ porphyrins were detected in fraction 6, and all homologous series identified are listed in Table S-6, Supporting Information.

Identification of "Acidic" Porphyrins. The addition of two oxygen atoms ($N_4O_3{}^{51}V$) was only observed in fraction 9, where formic acid was added to the eluent to displace acidic species from the amine-based stationary phase. Oxygen in carboxylic acid moieties increase the strength of adsorption on amine-based stationary phase and require elution with formic acid.[39] Elution of fraction 9 with 5% (by volume) formic acid identified $N_4O_3V_1$ porphyrins with DBE 19 and 20, which correspond to the addition of one DBE to the two most abundant $N_4O_1V_1$ types. This increase in DBE and elution of $N_4O_3V_1$ porphyrins along with naphthenic acids in fraction 9 suggest the presence of carboxylic acid-functionalized porphyrin structures (Table S-7, Supporting Information).[17]

CONCLUSIONS

Here, we present selective fractionation and separation of nickel and vanadyl porphyrins from a heavily weathered asphalt volcano sample based on adsorption and sequential elution on primary secondary amine stationary phase coupled to positive-ion electrospray ionization FT-ICR mass spectrometry. Chromatographic optimization of the separation with porphyrin model compounds combined with UV−vis absorption at characteristic porphyrin wavelengths and positive-ion electrospray FT-ICR MS provides elemental composition assignment confirmed by isotopic fine structure for both vanadyl and nickel porphyrins within the same sample. Secondary purification based on weak cation exchange for the nickel fraction increases the signal-to-noise ratio greater than 10-fold and extends the structural diversity of nickel porphyrins up to DBE 26. Oxygen-containing and sulfur-containing vanadyl porphyrins are

dx.doi.org/10.1021/ac502672b | Anal. Chem. 2014, 86, 10708−10715

identified, and we propose chromatographic evidence of carboxylic acid incorporation in porphyrins that are retained on PSA until the mobile phase composition is modified with formic acid. This method can be applied to all crude oils, and future studies will apply tandem mass spectrometry to further interrogate the structure of novel porphyrins.

■ ASSOCIATED CONTENT

Supporting Information

A complete description of all experimental methods, instrumental parameters, and detailed elemental composition assignment. This material is available free of charge via the Internet at http://pubs.acs.org.

■ AUTHOR INFORMATION

Corresponding Author

*Phone: +1 850 644 4809. Fax: +1 850 644 1366. E-mail: mckenna@magnet.fsu.edu.

Notes

The authors declare no competing financial interest.

■ ACKNOWLEDGMENTS

The authors thank Nathan K. Kaiser, Christopher L. Hendrickson, Gregory T. Blakney, and John P. Quinn for design and maintenance of the 9.4 T instrument, Ryan P. Rodgers and Winston K. Robbins for helpful discussions, and Alan G. Marshall for continued support. The authors thank Vincent Salters for access to the UV−vis spectrophotometer. Il Duomo samples were provided by David L. Valentine, Christopher M. Reddy, Christoph Aeppli, and Karin T. Lemkau. This work was supported by NSF Division of Materials Research through DMR-1157490, BP/The Gulf of Mexico Research Initiative to the Deep-C Consortium, and the State of Florida.

■ REFERENCES

(1) Treibs, A. *Justus Liebigs Ann. Chem.* **1935**, *517*, 172−196.
(2) Treibs, A. *Justus Liebigs Ann. Chem.* **1935**, *520*, 144−150.
(3) Callot, H. J.; Ocamp, R., Kadish, K. M.; Smith, K. M.; Guilard, R., Eds.; Academic Press: New York, 2000.
(4) Czernuszewicz, R. S. *J. Porphyrins Phthalocyanines* **2000**, *4*, 426−431.
(5) Barwise, A. J. G. *Energy Fuels* **1990**, *4*, 647−652.
(6) Baker, E. W.; Louda, J. W.; Orr, W. L. *Org. Geochem.* **1987**, *11*, 303−309. Szymczak-Zyla, M.; Kowalewska, G.; Louda, J. W. *Mar. Chem.* **2011**, *125*, 39−48.
(7) Ocampo, R.; Riva, A.; Trendel, J. M.; Riolo, J.; Callot, H. J.; Albrecht, P. *Energy Fuels* **1993**, *7*, 191−193.
(8) Altgelt, K. H.; Boduszynski, M. M. *Composition and Analysis of Heavy Petroleum Fractions*; CRC Press: New York, 1994.
(9) McKenna, A. M.; Williams, J. T.; Putman, J. C.; Aeppli, C.; Reddy, C. M.; Valentine, D. L.; Lemkau, K. L.; Kellerman, M. Y.; Savory, J. J.; Kaiser, N. K.; Marshall, A. G.; Rodgers, R. P. *Energy Fuels* **2014**, *28*, 2454−2464.
(10) Grigsby, R. D.; Green, J. B. *Energy Fuels* **1997**, *11*, 602−609.
(11) Pearson, C. D.; Green, J. B. *Energy Fuels* **1993**, *7*, 338−346.
(12) Peters, K. E.; Walters, C. C.; Moldowan, J. M. *The Biomarker Guide, Volume I: Biomarkers and Isotopes in the Environment and Human History*; Cambridge University Press: New York, 2005; Vol. *1*.
(13) Fleischer, E. B. *J. Am. Chem. Soc.* **1963**, *85*, 146−148.
(14) Rankin, J. G.; Czernuszewicz, R. S.; Lash, T. D. *Org. Geochem.* **1995**, *23*, 419−427. Czernuszewicz, R. S.; Rankin, J. G.; Lash, T. D. *Inorg. Chem.* **1996**, *35*, 199−209. Rankin, J. G.; Cantu, R.; Czernuszewicz, R. S.; Lash, T. D. *Org. Geochem.* **1999**, *30*, 201−208. Boggess, J. M.; Czernuszewicz, R. S.; Lash, T. D. *Org. Geochem.* **2002**, *33*, 1111−1126. Czader, A.; Czernuszewicz, R. S. *Org. Geochem.* **2007**, *38*, 250−266.
(15) Dechaine, G. P.; Gray, M. R. *Energy Fuels* **2010**, *24*, 2795−2808. Marcano, F.; Flores, R.; Chirinos, J.; Ranaudo, M. A. *Energy Fuels* **2011**, *25*, 2137−2141. Yin, C.-X.; Tan, X.; Mullen, K.; Stryker, J. M.; Gray, M. R. *Energy Fuels* **2008**, *22*, 2465−2469.
(16) Hajibrahim, S. K.; Quirke, J. M. E.; Eglinton, G. *Chem. Geol.* **1981**, *32*, 173−188. Fish, R. H.; Komlenic, J. J.; Wines, B. K. *Anal. Chem.* **1984**, *56*, 2452−2460. Marquez, N.; Ysambertt, F.; De la Cruz, C. *Anal. Chim. Acta* **1999**, *395*, 343−349. Yin, C.-X.; Stryker, J. M.; Gray, M. R. *Energy Fuels* **2009**, *23*, 2600−2605.
(17) Zhao, X.; Liu, Y.; Xu, C.; Yan, Y.; Zhang, Y.; Zhang, Q.; Zhao, S.; Chung, K.; Gray, M. R.; Shi, Q. *Energy Fuels* **2013**, *27*, 2874−2882.
(18) Gallegos, E. J.; Sundararaman, P. *Mass Spectrom. Rev.* **1985**, *4*, 55−85. Johnson, J. V.; Britton, E. D.; Yost, R. A.; Quirke, J. M. E.; Cuesta, L. L. *Anal. Chem.* **1986**, *58*, 1325−1329. Frakman, Z.; Ignasiak, T. M.; Montgomery, D. S.; Strausz, O. P. *AOSTRA J. Res.* **1988**, *4*, 171−179. Faramawy, S.; El-Sabagh, S. M.; Moustafa, Y. M.; El-Naggar, A. Y. *Petr. Sci. Technol.* **2010**, *28*, 603−617.
(19) Qian, K.; Edwards, K. E.; Mennito, A. S.; Walters, C. C.; Kushnerick, J. D. *Anal. Chem.* **2010**, *82*, 413−419.
(20) Qian, K.; Mennito, A. S.; Edwards, K. E.; Ferrughelli, D. T. *Rapid Commun. Mass Spectrom.* **2008**, *22*, 2153−2160.
(21) Rodgers, R. P.; Hendrickson, C. L.; Emmett, M. R.; Marshall, A. G.; Greaney, M. A.; Qian, K. *Can. J. Chem.* **2001**, *79*, 546−551.
(22) McKenna, A. M.; Purcell, J. M.; Rodgers, R. P.; Marshall, A. G. *Energy Fuels* **2009**, *23*, 2122−2128.
(23) Liao, Z.; Zhao, J.; Creux, P.; Yang, C. *Energy Fuels* **2009**, *23*, 6272−6274.
(24) Rodgers, R. P.; Marshall, A. G. Petroleomics: Advanced Characterization of Petroleum Derived Materials by Fourier Transform Ion Cyclotron Resonance Mass Spectrometry (FT-ICR MS). In *Asphaltenes, Heavy Oils and Petroleomics*, Mullins, O. C.; Sheu, E. Y.; Hammami, A.; Marshall, A. G., Eds.; Springer: New York, 2006; Chapter 3, pp 63−93. Rodgers, R. P.; Schaub, T. M.; Marshall, A. G. *Anal. Chem.* **2005**, 77. Rodgers, R. P.; McKenna, A. M. *Anal. Chem.* **2011**, *83*, 4665−4687. McKenna, A. M.; Blakney, G. T.; Xian, F.; Glaser, P. B.; Rodgers, R. P.; Marshall, A. G. *Energy Fuels* **2010**, *24*, 2939−2946. McKenna, A. M.; Donald, L. J.; Fitzsimmons, J. E.; Juyal, P.; Spicer, V.; Standing, K. G.; Marshall, A. G.; Rodgers, R. P. *Energy Fuels* **2013**, *271*246−1256. McKenna, A. M.; Marshall, A. G.; Rodgers, R. P. *Energy Fuels* **2013**, *27*, 1257−1267. McKenna, A. M.; Purcell, J. M.; Rodgers, R. P.; Marshall, A. G. *Energy Fuels* **2010**, *24*, 2929−2938. Podgorski, D. C.; Corilo, Y. E.; Nyadong, L.; Lobodin, V. V.; Bythell, B. J.; Robbins, W. K.; McKenna, A. M.; Marshall, A. G.; Rodgers, R. P. *Energy Fuels* **2013**, *27*, 1268−1276.
(25) Xu, H. L. S. *J. Chromatogr.* **1992**, *607*, 139−144.
(26) Robb, D. B.; Blades, M. W. *J. Am. Soc. Mass Spectrom.* **2006**, *17*, 130−138.
(27) Zhan, D.; Fenn, J. B. *Int. J. Mass Spectrom.* **2000**, *194*, 197−208.
(28) Valentine, D. L.; Reddy, C. M.; Farwell, C.; Hill, T. M.; Pizarro, O.; Yoerger, D. R.; Camilli, R.; Nelson, R. K.; Peacock, E. A.; Bagby, S. C.; Clarke, B. A.; Roman, C. N.; Soloway, M. *Nat. Geosci.* **2010**, *3*, 345−348.
(29) Cantu, R.; Stencel, J. R.; Czernuszewicz, R. S.; Jaffe, P. R.; Lash, T. D. *Environ. Sci. Technol.* **2000**, *34*, 192−198.
(30) Medforth, C. J.; Senge, M. O.; Smith, K. M.; Sparks, L. D.; Shelnutt, J. A. *J. Am. Chem. Soc.* **1992**, *114*, 9859−9869.
(31) Emmett, M. R.; White, F. M.; Hendrickson, C. L.; Shi, S. D.-H.; Marshall, A. G. *J. Am. Soc. Mass Spectrom.* **1998**, *9*, 333−340.
(32) Shaffer, S. A.; Prior, D. C.; Anderson, G. A.; Udseth, H. R.; Smith, R. D. *Anal. Chem.* **1998**, *70*, 4111−4119.
(33) Kaiser, N. K.; Quinn, J. P.; Blakney, G. T.; Hendrickson, C. L.; Marshall, A. G. *J. Am. Soc. Mass Spectrom.* **2011**, *22*, 1343−1351.
(34) Blakney, G. T.; Hendrickson, C. L.; Marshall, A. G. *Int. J. Mass Spectrom.* **2011**, *306*, 246−252.
(35) Beu, S. C.; Blakney, G. T.; Quinn, J. P.; Hendrickson, C. L.; Marshall, A. G. *Anal. Chem.* **2004**, *76*, 5756−5761.

(36) Xian, F.; Corilo, Y. E.; Hendrickson, C. L.; Marshall, A. G. *Int. J. Mass Spectrom.* **2012**, *325*−*327*, 67−72. Xian, F.; Hendrickson, C. L.; Blakney, G. T.; Beu, S. C.; Marshall, A. G. *Anal. Chem.* **2010**, *82*, 8807−8812.
(37) Marshall, A. G.; Hendrickson, C. L.; Jackson, G. S. *Mass Spectrom. Rev.* **1998**, *17*, 1−35.
(38) Chen, Z.; Dong, F.; Xu, J.; Liu, X.; Cheng, Y.; Liu, N.; Tao, Y.; Zheng, Y. *Chirality* **2014**, *26*, 114−120.
(39) Qian, K.; Robbins, W. K.; Hughey, C. A.; Cooper, H. J.; Rodgers, R. P.; Marshall, A. G. *Energy Fuels* **2001**, *15*, 1505−1511.